

**Supplemental Table I. Quantification of Meiosis in *dhc-1(RNAi)***

	Wild type	<i>unc-116</i> ( <i>rh24sb79</i> )	<i>dhc-1 (RNAi)</i>	<i>unc-116</i> ( <i>rh24sb79</i> ); <i>dhc-1 (RNAi)</i>
Time from Exit of Spermatheca (Esp) to second				
Polar Body Extrusion (PBE) (min)	28.9 (n=1)	25.1 ± 0.7 (n=4)	28.5 ± 1.6 (n=7)	24.8 ± 1.0 (n=7)
<b>Meiosis I</b>				
Metaphase spindle length (µm)	7.2 ± 0.2 (n=13)	7.1 ± 0.2 (n=11)	7.6 ± 0.3 (n=20)	6.8 ± 0.3 (n=11)
Distance from metaphase spindle to cortex (µm)	0.9 ± 0.2 (n=11)	5.6 ± 0.6 (n=13)	1.0 ± 0.2 (n=20)	5.0 ± 0.7 (n=12)
Time from ES <sub>p</sub> to begin of spindle shortening spindle (min)	6.7 ± 0.6 (n=11)	3.9 ± 0.4 (n=11)	5.1 ± 0.4 (n=15)	3.8 ± 0.4 (n=7)
Time from ES <sub>p</sub> to spindle rotation/late translocation (min)	8.1 ± 0.6 (n=13)	5.7 ± 0.5 (n=12)	6.5 ± 0.9 (n=4)	6.9 (n=1)
Time between spindle shortening and rotation/late translocation (min)	1.7 ± 0.2 (n=12)	1.8 ± 0.2 (n=13)	2.0 ± 0.4 (n=8)	2.7 (n=1)
Time of PBE (min)	16.5 ± 1.3 (n=6)	12.6 ± 0.9 (n=6)	13.5 ± 0.6 (n=10)	11.6 ± 0.6 (n=7)
<b>Meiosis II</b>				
Metaphase spindle length (µm)	5.9 ± 0.4 (n=8)	6.1 ± 0.3 (n=6)	6.6 ± 0.3 (n=15)	6.4 ± 0.2 (n=12)
Distance from metaphase spindle to cortex (µm)	1.1 ± 0.2 (n=7)	3.2 ± 0.6 (n=7)	0.9 ± 0.3 (n=13)	4.4 ± 1.0 (n=8)
Time from ES <sub>p</sub> to begin of spindle shortening spindle (min)	6.5 ± 0.9 (n=8)	4.7 ± 0.3 (n=6)	6.0 ± 0.25 (n=12)	5.4 ± 0.5 (n=8)
Time from ES <sub>p</sub> to spindle rotation/late translocation (min)	7.9 ± 0.9 (n=8)	6.0 ± 0.3 (n=8)	7.8 ± 0.4 (n=4)	7.2 ± 0.4 (n=3)
Time between spindle shortening and rotation/late translocation (min)	1.9 ± 0.2 (n=7)	1.6 ± 0.4 (n=6)	2.0 ± 0.2 (n=4)	1.8 ± 0.3 (n=3)
Time of PBE (min)	12.9 ± 0.6 (n=2)	14.1 ± 1.2 (n=7)	15.3 ± 1.2 (n=10)	13.4 ± 0.4 (n=9)

**ES<sub>p</sub>=Exit from the Spermatheca**

**PBE= Polar Body Extrusion**

**Supplemental Figure 1. *dhc-1 (RNAi)* results in abnormal polar body extrusion.** (A)

Examples of normal (wild-type and *unc-116*) and abnormal (*dhc-1(RNAi)* and *unc-116;dhc-1(RNAi)*) polar body extrusion. Images are of GFP:tubulin in meiotic embryos at the time of polar body extrusion. In the middle row the cell cortex and ectopic furrows (*dhc-1(RNAi)* and *unc-116;dhc-1(RNAi)*) have been highlighted for clarity. (B) Example of two meiosis II spindle completing anaphase II in *unc-116;dhc-1(RNAi)*. Images are of mcherry:histone H2B (top row) and GFP-tubulin (bottom row). T=0 is exit from the spermatheca and the cell cortex has been highlighted for clarity. White arrowheads point to the four pronuclei that formed as a result of two meiosis II spindles completing anaphase in one embryo.

**Supplemental Figure 2. Dynein regulators localize to meiotic spindle poles during**

**rotation.** Images of GFP: DNC-2 (A), GFP:DYRB-1 (B), and GFP:DNC-1 (C) within a meiotic embryo are shown from representative time-lapse sequences of wild-type worms. The cell cortex was highlighted in each image for clarity. Drawings corresponding to each image are included only to demonstrate spindle orientation for clarity, but are not drawn to scale and are not accurate replications of the images. 0 sec is the start of rotation. (A) GFP:DNC-2 faintly localized across the meiotic spindle prior to spindle shortening (T= -120 sec). 45-30 seconds prior to the start of rotation, GFP:DNC-2 accumulated on meiotic spindle poles and remained on meiotic spindle poles after rotation (T = +60 sec). (B) GFP:DYRB-1 faintly localized across the meiotic spindle prior to spindle rotation. 45-30 seconds prior to the start of rotation, GFP:DYRB-1 began

to accumulate on meiotic spindle poles and remained on meiotic spindle poles after rotation (T = +30 sec). (C) GFP:DNC-1 faintly localized across the meiotic spindle prior to spindle rotation (T=-60sec). 45-30 seconds prior to the start of rotation, GFP:DNC-1 began to accumulate on meiotic spindle poles and remained on meiotic spindle poles after rotation (T = +30 sec). (D) Immunostaining of anti-DNC-1 in fixed wild-type embryos, co-stained with anti-tubulin (TUB) and DAPI to visualize the chromosomes. The top row is a metaphase spindle with DNC-1 faintly localized throughout the spindle. The middle row is a rotated spindle prior to chromosome segregation with anti-DNC-1 localized to the spindle poles. The bottom row is an anaphase spindle with DNC-1 localized to the spindle poles. (E) Immunostaining of anti-LIN-5 in fixed wild-type embryos, co-stained with anti-tubulin (TUB) and DAPI to visualize the chromosomes. The top row is a metaphase spindle with LIN-5 localized throughout the spindle. The middle row is a rotated spindle prior to chromosome segregation with anti-LIN-5 localized brightly to the spindle poles and throughout the spindle. The bottom row is an anaphase spindle with LIN-5 localized to the spindle midzone. Scale Bars, (A-C) 10  $\mu$ m, (D-E) 5  $\mu$ m.

**Supplemental Figure 3. In the absence of KCA-1, Dynein regulators accumulate on meiotic spindle poles during late translocation.** Images GFP: DNC-2 (A) and GFP:DYRB-1 (B) within a meiotic embryo are shown from representative time-lapse sequences of a *kca-1(RNAi)* worms. The cell cortex was highlighted in each image for clarity. Drawings corresponding to each image are included only to demonstrate spindle orientation for clarity, but are not drawn to scale and are not accurate replications of the images. 0 sec is the start of late translocation. (A) GFP:DNC-2 faintly localized across

the meiotic spindle prior to spindle shortening (T= -120 sec). 45-30 seconds prior to the start of late spindle translocation, GFP:DNC-2 began to accumulate on meiotic spindle poles and remained on meiotic spindle poles after late translocation (T = +60 sec). (B) GFP:DYRB-1 faintly localized across the meiotic spindle prior to spindle shortening (T= -120 sec). 45-30 seconds prior to the start of late spindle translocation, GFP:DYRB-1 began to accumulate on meiotic spindle poles and remained on meiotic spindle poles after late translocation (T = +60 sec). Scale Bars, 10  $\mu$ m.

**Supplemental Figure 4. Dynein localizes to the spindle cortex and microtubules extending from the spindle to the cortex.** (A, B, C) Three representative time-lapse sequences of GFP:DHC-1 in wild-type meiotic embryos during rotation. White arrowheads point towards GFP:DHC-1 localized to microtubules extending from the meiotic spindle to the cell cortex during spindle rotation. White arrows point towards GFP:DHC-1 localized in a patch-like area at the cell cortex during spindle rotation. 0 sec is the initiation of rotation. (D) Immunostaining of anti-DHC-1 in fixed wild-type embryos, co-stained with anti-tubulin (TUB) and DAPI to visualize the chromosomes. White arrows point towards anti-DHC-1 localized to the cell cortex. All scale bars; 5 $\mu$ m.

**Video 1. Meiotic spindle movements during meiosis I in a wild-type embryo imaged with GFP:tubulin.**

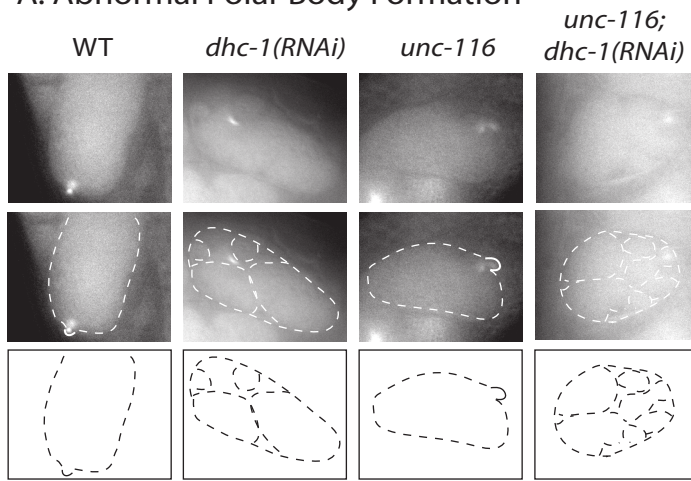
**Video 2. Meiotic spindle movements during meiosis I in a *dhc-1(RNAi)* embryo imaged with GFP:tubulin.**

**Video 3. Meiotic spindle movements during meiosis I in an *unc-116* embryo imaged with GFP:tubulin.**

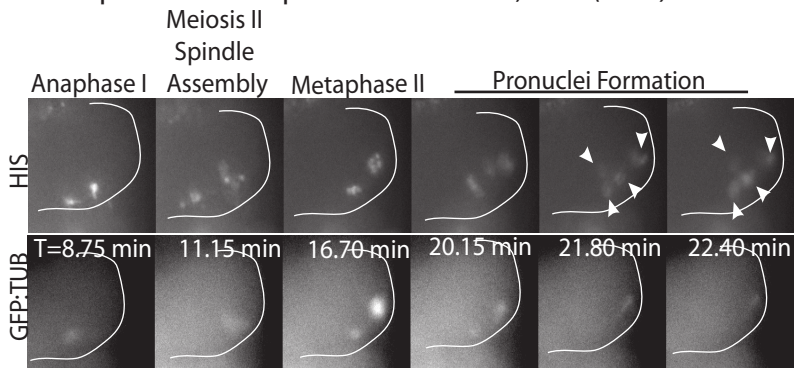
**Video 4. Meiotic spindle movements during meiosis I in an *unc-116;dhc-1(RNAi)* embryo imaged with GFP:tubulin.**

# Supplemental Figure 1

## A. Abnormal Polar Body Formation

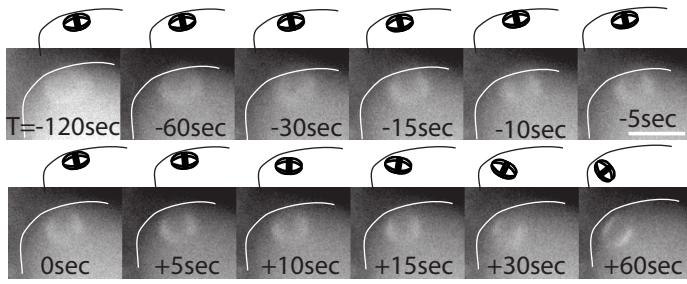


## B. Multiple Meiosis II Spindles in *unc-116;dhc-1(RNAi)*

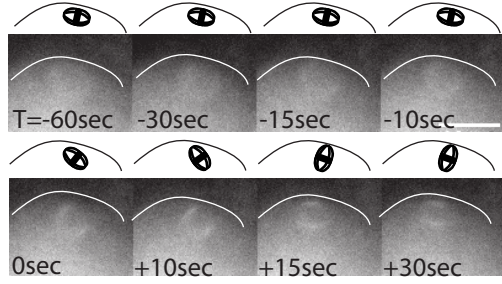


# Supplemental Figure 2

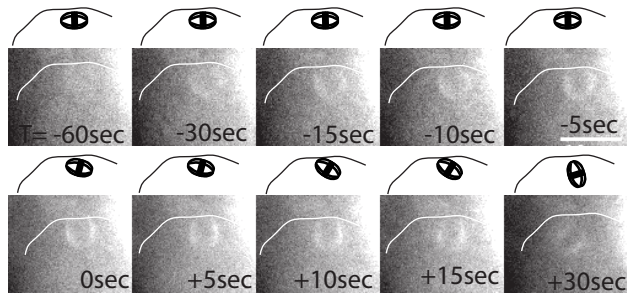
## A. GFP:DNC-2



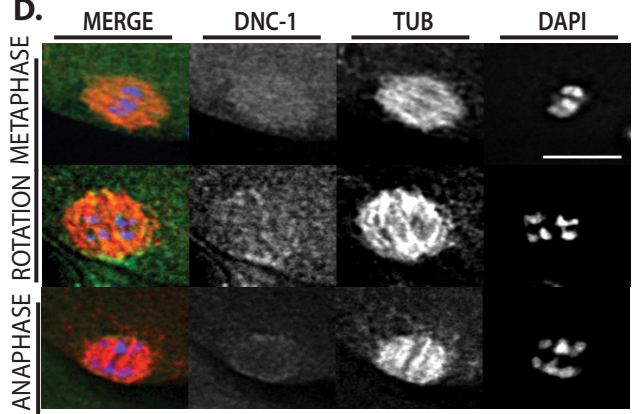
## B. GFP:DYRB-1



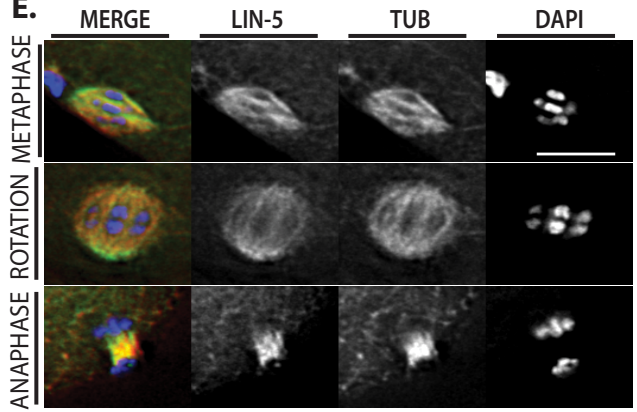
## C. GFP:DNC-1



## D.

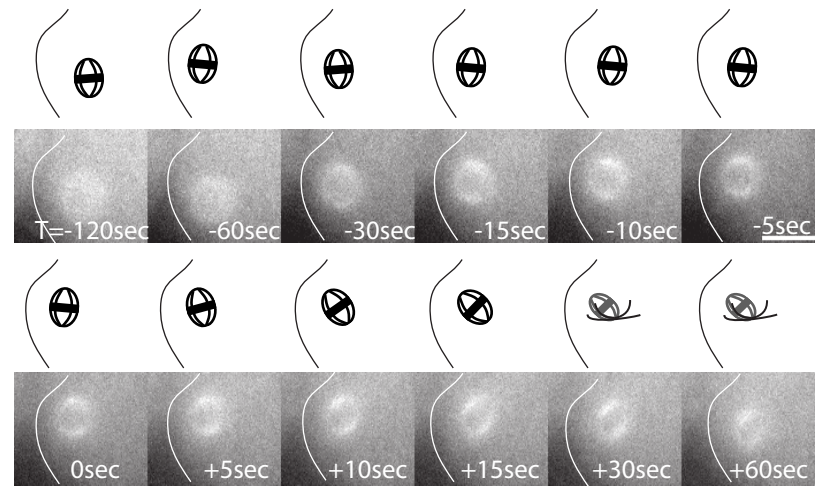


## E.

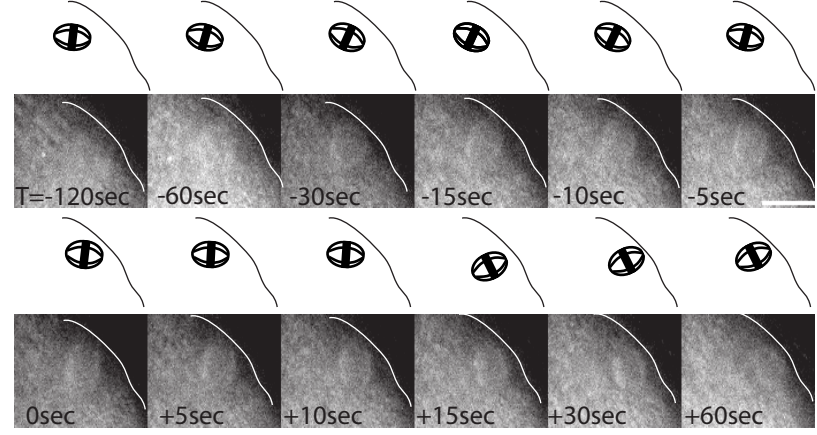


**Supplemental Figure 3.**

**A. GFP:DNC-2; *kca-1(RNAi)***



**B. GFP:DYRB-1; *kca-1(RNAi)***





**Supplemental Figure 4.**

